Supplementary Materials

A high-performance quasi-solid-state supercapacitor diode for flexible logic gate

Dongmei Zhai[#], Zefeng Yan[#], Keyi Dong, Weiyang Tang, Quanhu Sun, Xiao Li, Jiaxin Yang, Tian Lv, Tao Chen[*]

Shanghai Key Lab of Chemical Assessment and Sustainability, School of Chemical Science and Engineering, Tongji University, Shanghai 200092, China.
[#]Equally contributed to this work.

[*]**Correspondence to:** Prof. Tao Chen, Shanghai Key Lab of Chemical Assessment and Sustainability, School of Chemical Science and Engineering, Tongji University, Shanghai 200092, China. E-mail: tchen@tongji.edu.cn

Experimental section

1. Materials

Ammonium molybdate tetrahydrate ($(NH_4)_6Mo_7O_{24}\cdot 4H_2O$), nitric acid ($HNO_3$), absolute ethanol ($C_2H_5OH$) and L(+)–tartaric acid ($C_4H_6O_6$, 99.0%) were purchased from Aladdin. All chemicals were used without further purification. Deionized water was used for the preparation of samples.

2. Synthesis of MoO_x Nanobelts

MoO_x nanobelts were synthesized by a one–step hydrothermal method. First, $(NH_4)_6Mo_7O_{24}\cdot 4H_2O$ (825 mg, 99.9%, Aladdin, Shanghai) and L(+)–tartaric acid (400 mg, 99%, Aladdin, Shanghai) were dissolved in deionized water (50 mL), the achieved solution was stirred under a speed of 500 rpm at room temperature for 30 min. Then, nitric acid (1 mL, AR, Sinopharm, Shanghai) was added to the above solution, and stirring under a speed of 500 rpm at room temperature for 10 min. After that, the mixed solution was transferred to a Teflon–lined stainless–steel autoclave and kept at 180 °C for 24 h. Finally, a milky white precipitate was collected by centrifugation (8000 rpm), followed by washing with ethanol and DI water three times, respectively. The product was dried in a vacuum oven at 60 °C for 24 h for further use.

3. Preparation of PVA/H_3PO_4 Electrolytes

Polyvinyl alcohol (PVA, 10 wt%, Aladdin, Shanghai) was first added to deionized water (10 mL) with stirring under a speed of 600 rpm, and a transparent solution was achieved after heating at 80 °C for 2 h. After the PVA aqueous solution was cooled to room temperature, 120 μL H_3PO_4 (AR, MACKLIN, Shanghai) was added. The other electrolytes (H_2SO_4, AR, Sinopharm, Shanghai; $HClO_4$, GR, Sinopharm, Shanghai) were prepared by the same method, with adding the corresponding acid (0.2 M).

4. Electrochemical Measurements

The specific capacitance of the whole device (C) was calculated from GCD curves according to the equation [S1]:

$$C = \frac{I\Delta t}{m\Delta U} \qquad \text{(S1)}$$

where C(F g^{-1}) is the specific capacitance, I(A) is the discharge current, Δt (s) is the discharge time, m (g) is the mass of active material, and ΔU (V) is the potential window during the discharge process.

The rectification ratio I (RR_I) is calculated from CV curves according to the equation [S2]:

$$RR_I = \frac{\Delta I_1}{\Delta I_2} \qquad \text{(S2)}$$

where ΔI_1(A) is the current difference between redox peaks in the forward–direction voltage region (i.e., –0.95–0 V), and ΔI_2(A) is the current difference between redox peaks in the reverse–direction voltage region (i.e., electrochemical double–layer adsorption region, 0–0.95 V).

The rectification ratio II (RR_{II}) is calculated from GCD curves according to the equation [S3]:

$$RR_{II} = \frac{C_1}{C_2} \qquad \text{(S3)}$$

where C_1 is the capacitance in the forward–direction voltage region, and C_2 is the capacitance in the total voltage window.

The rectification ratio, calculated from the I–t curve, is the ratio of the absolute value of the current at the maximum applied voltage in the forward–direction voltage region to the absolute value of the current at the maximum applied voltage in the reverse–direction voltage region.

5. Theoretical Calculations.

All the theoretical calculations were based on the Density Functional Theory (DFT) and performed on Materials Studio 2019 by using Dmol3 module. The generalized gradient approximation (GGA) of the Perdew–Burke–Ernzerhof (PBE) functionals and Dual numerical additive polarization (DNP) basis set were adopted to conduct the geometry optimization and energy computation [S1, S2]. A 3×3×1 grid of k–points was generated by using the Monkhorst–Pack scheme to obtain the precise energy and structure. To reduce the interaction between adjacent layers, 20 Å vacuum spacing was set along the y–axis. The energy convergence accuracy, maximum stress, and maximum displacement are 1×10^{-5} Ha, 2×10^{-3} Ha/Å, and 5×10^{-3} Ha, respectively. The self–consistent field convergence accuracy is 1×10^{-6} Ha.

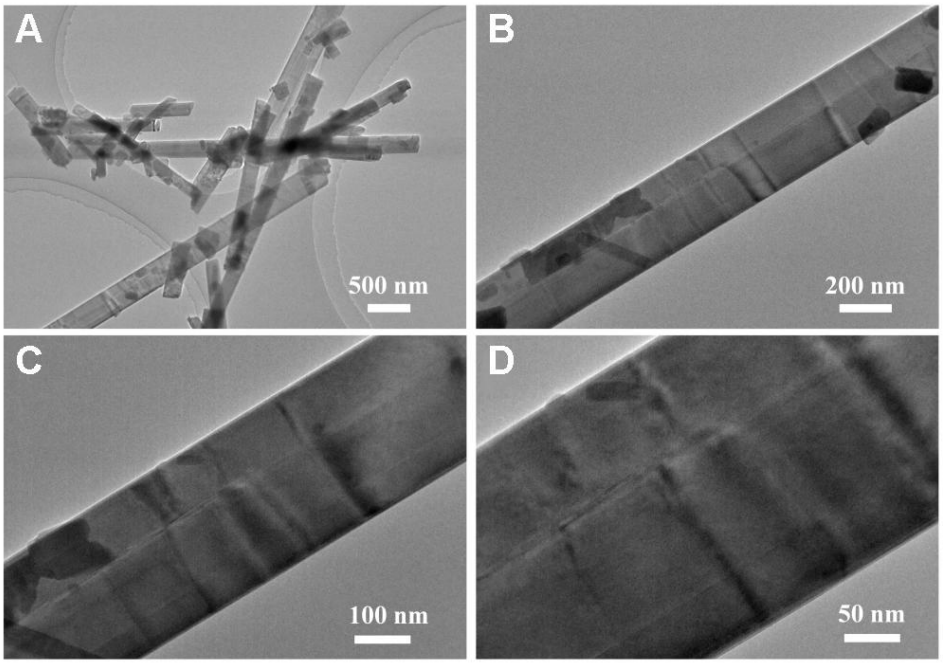

Supplementary Figure 1. (A) TEM image of MoO_x nanobelts; (B and C) TEM images of one MoOx nanobelts at different magnifications.

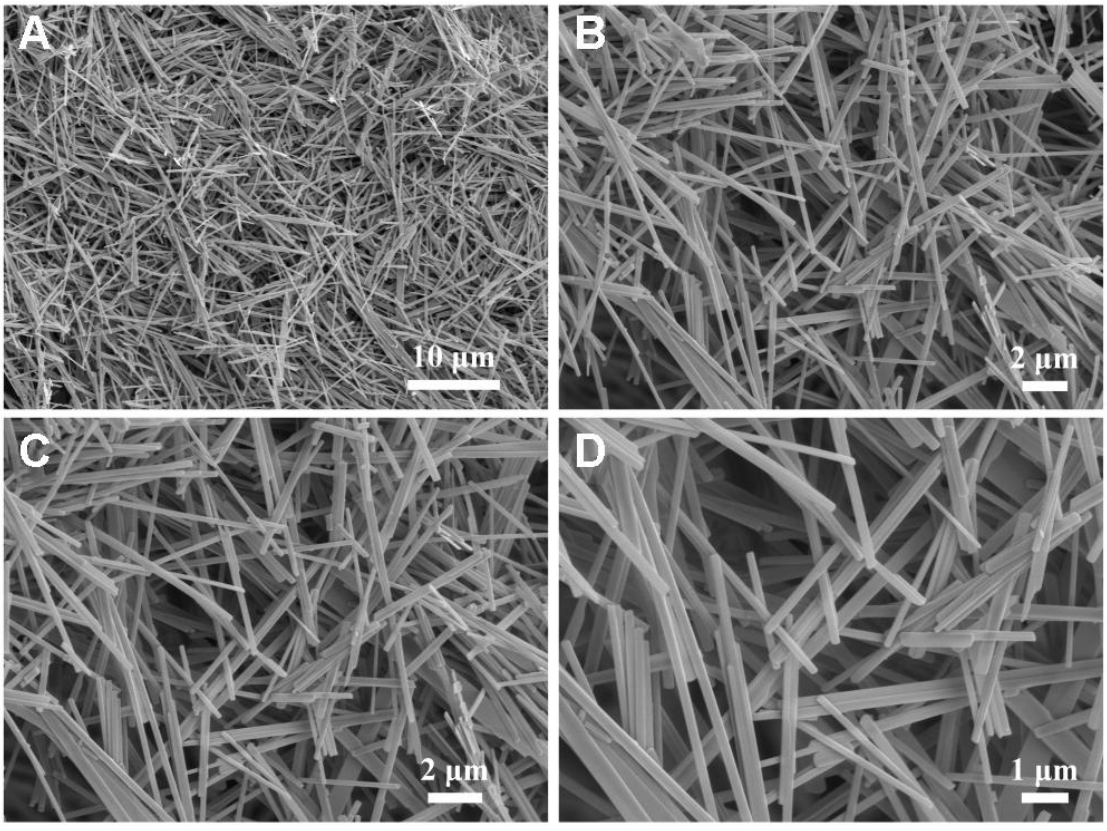

Supplementary Figure 2. (A-D) SEM images of MoO_x nanobelts at different magnifications.

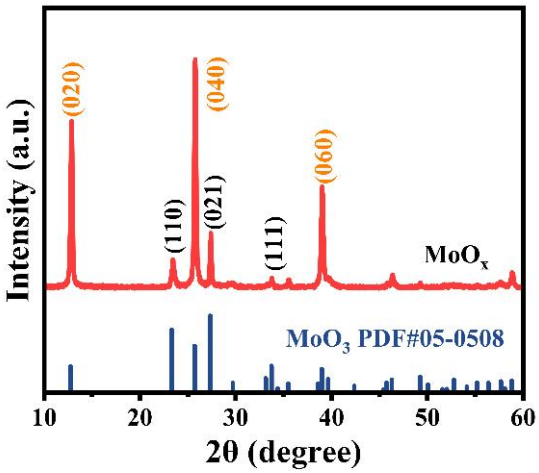

Supplementary Figure 3. XRD pattern of MoO_x nanobelts.

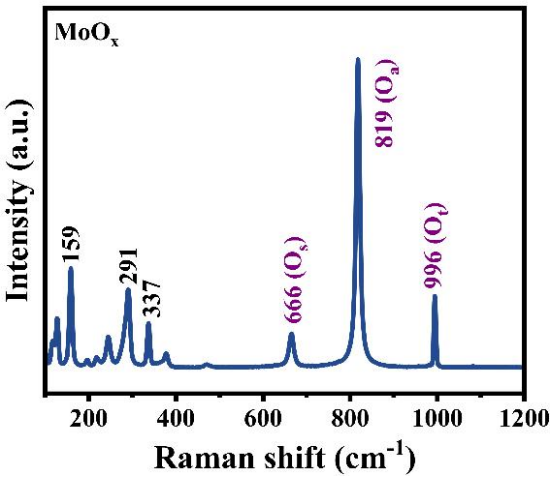

Supplementary Figure 4. Raman spectra of MoO_x nanobelts.

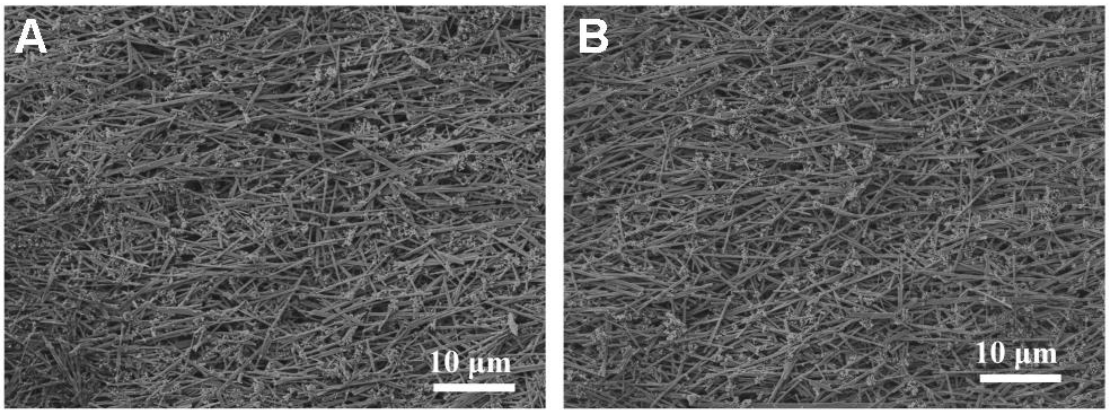

Supplementary Figure 5. SEM images of MoO_x/CNTs electrode after being bent to 135° for 1000 (A) and 2000 (B) cycles.

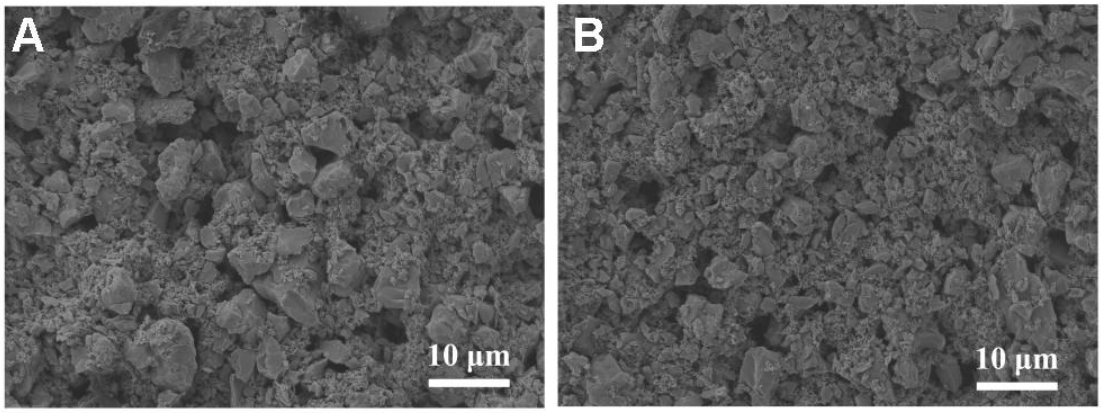

Supplementary Figure 6. SEM images of AC/CNTs electrode being bent to 135° for 1000 (A) and 2000 (B) cycles.

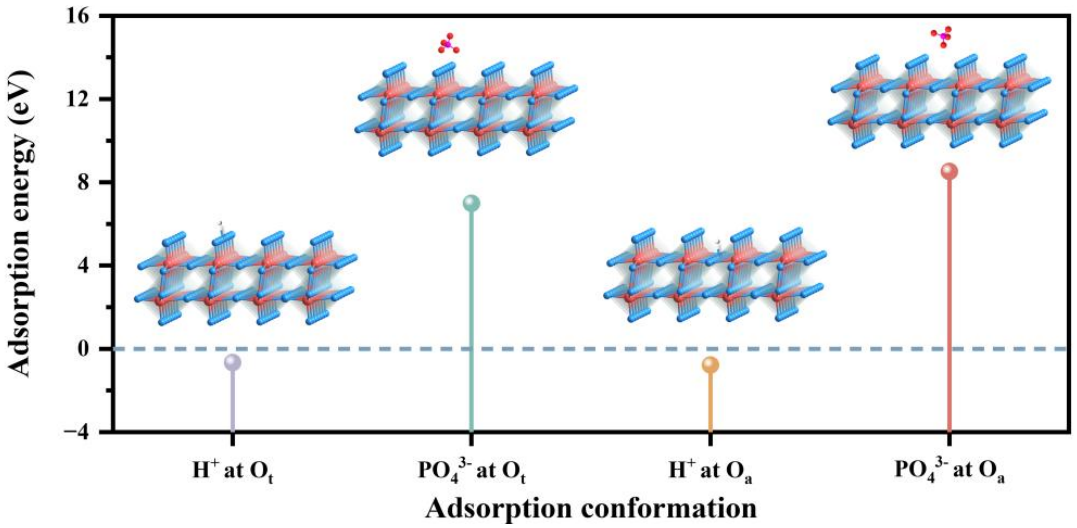

Supplementary Figure 7. The calculated adsorption energies of H^+ and PO_4^{3-} ions at various active sites on MoOx by DFT.

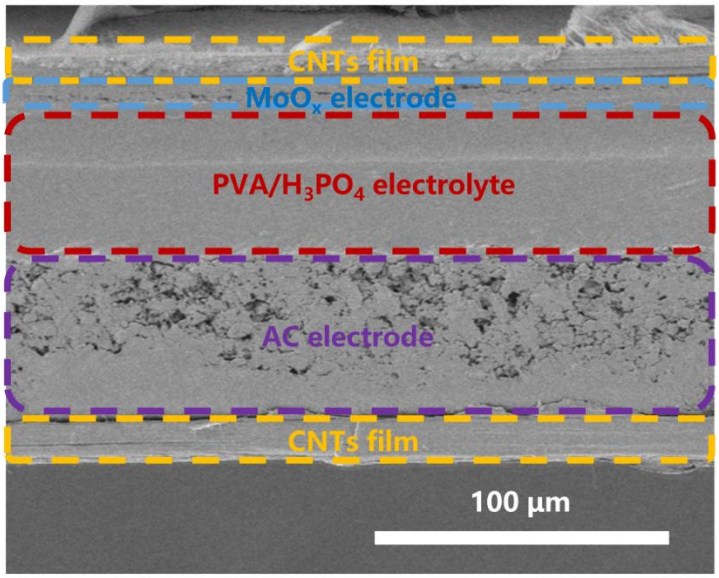

Supplementary Figure 8. Cross-sectional SEM image of the whole device ($CNTs/MoO_x$ // PVA/H_3PO_4 // CNTs/AC)

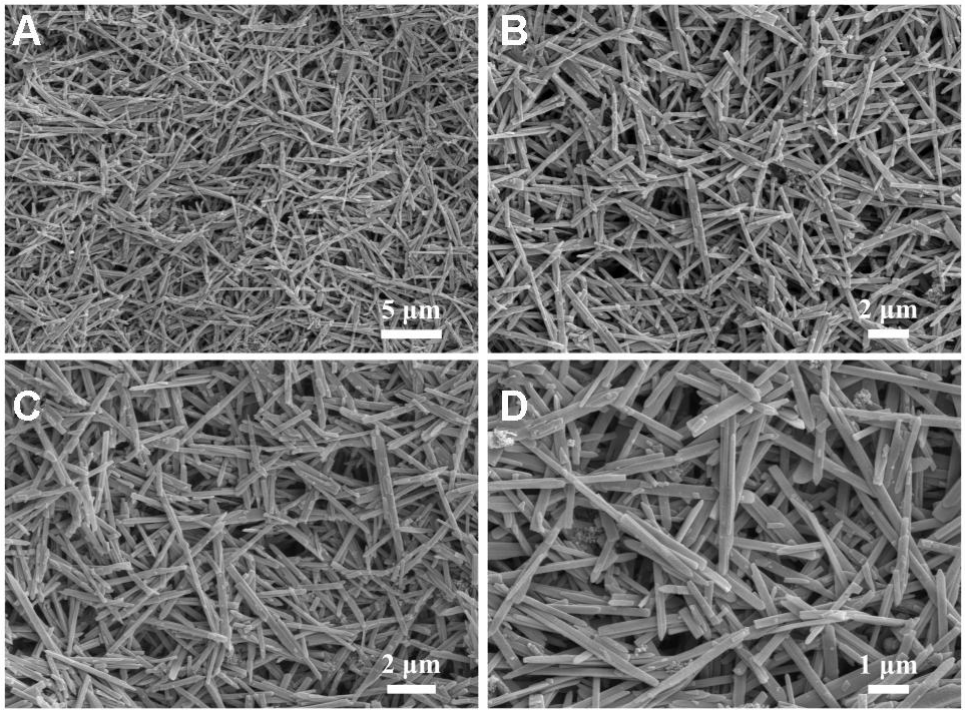

Supplementary Figure 9. (A-D) SEM images of MoO_x/CNTs electrode at different magnifications.

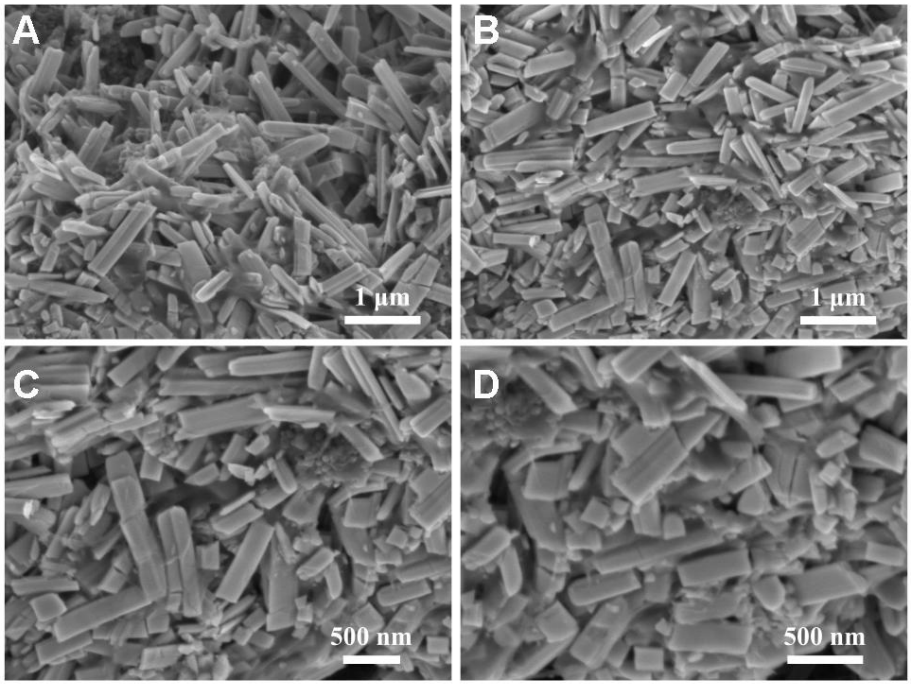

Supplementary Figure 10. (A-D) SEM images of MoO_x/CNTs electrode at different magnifications after cycling.

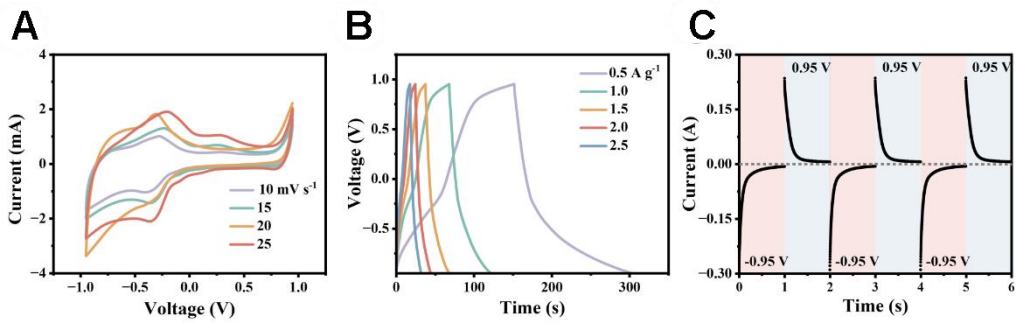

Supplementary Figure 11. Electrochemical and rectification electrochemical performances of the CAPode with using polymer electrolyte containing LiCl aqueous solution (0.2 M). (A) CV curves at different scan rates. (B) GCD curves at different current densities. (C) Chronoamperometry curves of CAPode under alternating voltage of ± 0.95 V, applied for 1 s.

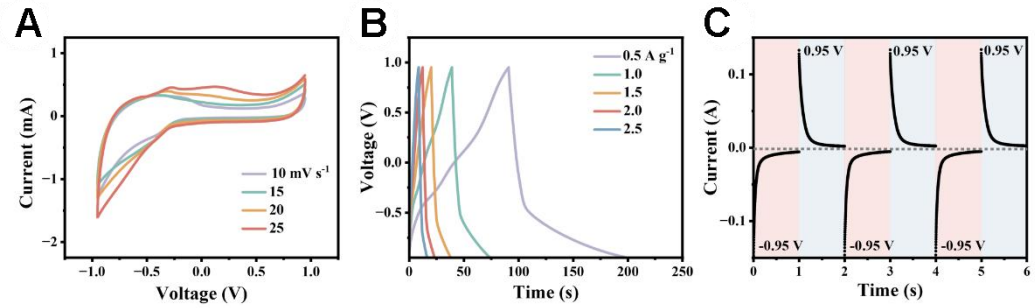

Supplementary Figure 12. Electrochemical and rectification electrochemical performances of the CAPode with using polymer electrolyte containing KOH aqueous solution (0.2 M). (A) CV curves at different scan rates. (B) GCD curves at different current densities. (C) Chronoamperometry curves of CAPode under alternating voltage of ± 0.95 V, applied for 1 s.

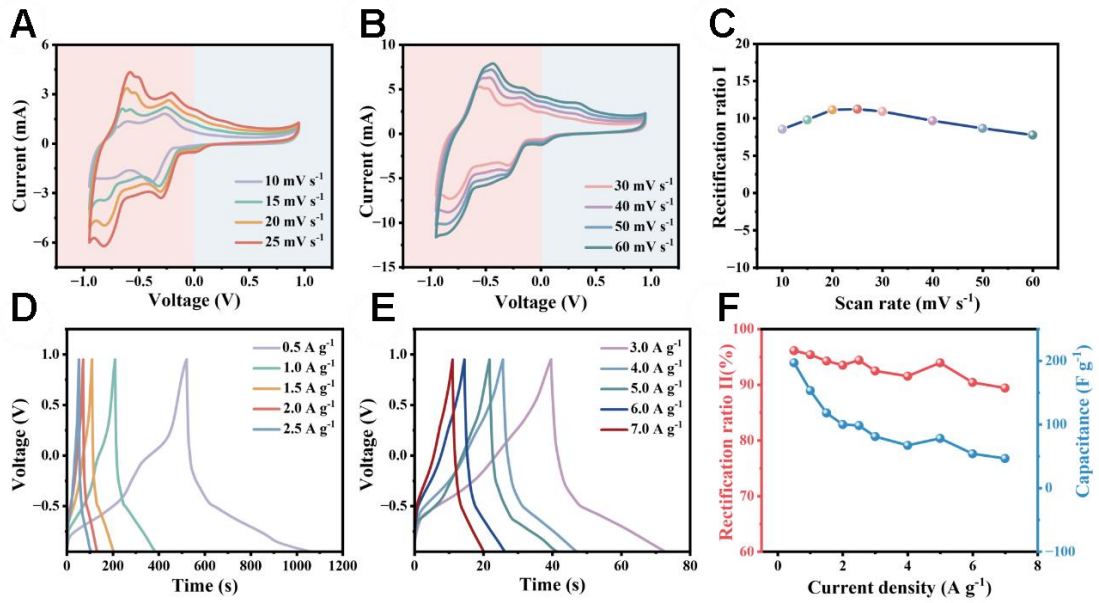

Supplementary Figure 13. Electrochemical and rectification electrochemical performances of the CAPode with using polymer electrolyte containing H_2SO_4 solution (0.2 M). (A, B) CV curves at different scan rates. (C) RR_I at different scan rates. (D, E) GCD curves at different current densities. (F) RR_{II} and specific capacitance at different current densities.

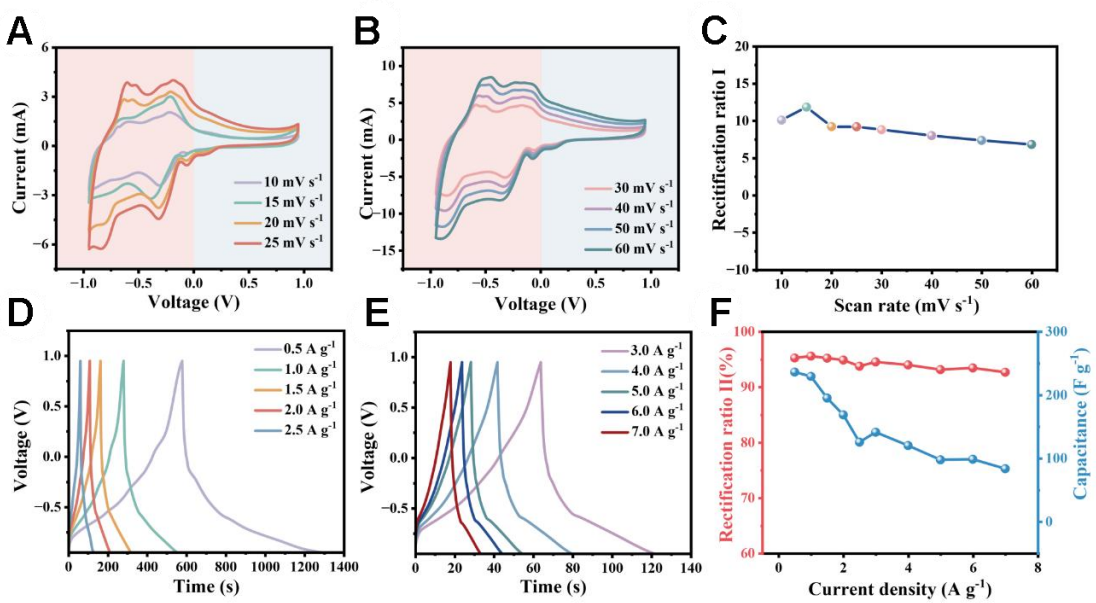

Supplementary Figure 14. Electrochemical and rectification electrochemical performances of the CAPode with using polymer electrolyte containing $HClO_4$ solution (0.2 M). (A, B) CV curves at different scan rates. (C) RR_I at different scan rates. (D, E) GCD curves at different current densities. (F) RR_{II} and specific capacitance at different current densities.

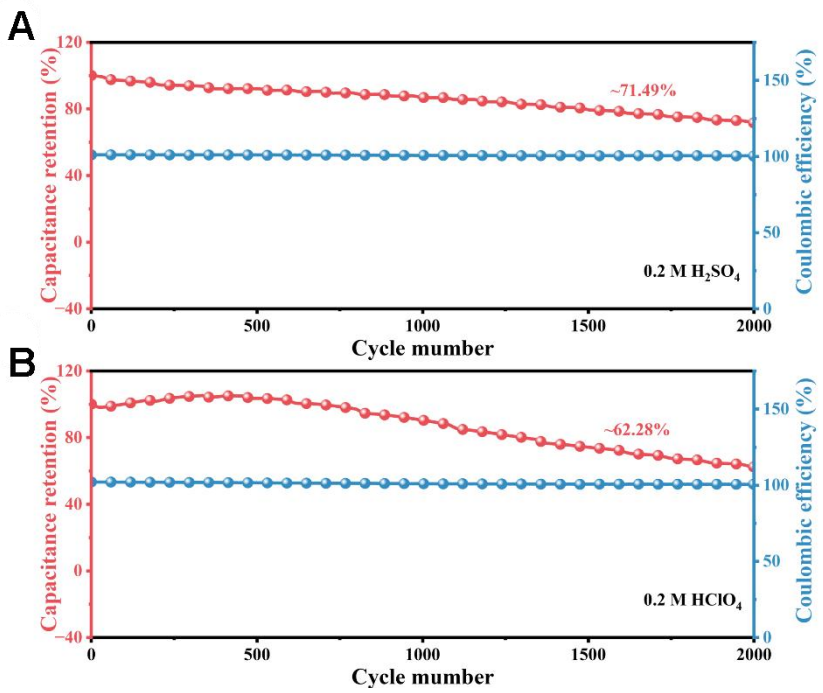

Supplementary Figure 15. Cycling stabilities of CAPode with using electrolytes of H_2SO_4 (A) and $HClO_4$ (B) aqueous solution under charge/discharge current density of 2 A g^{-1}, respectively.

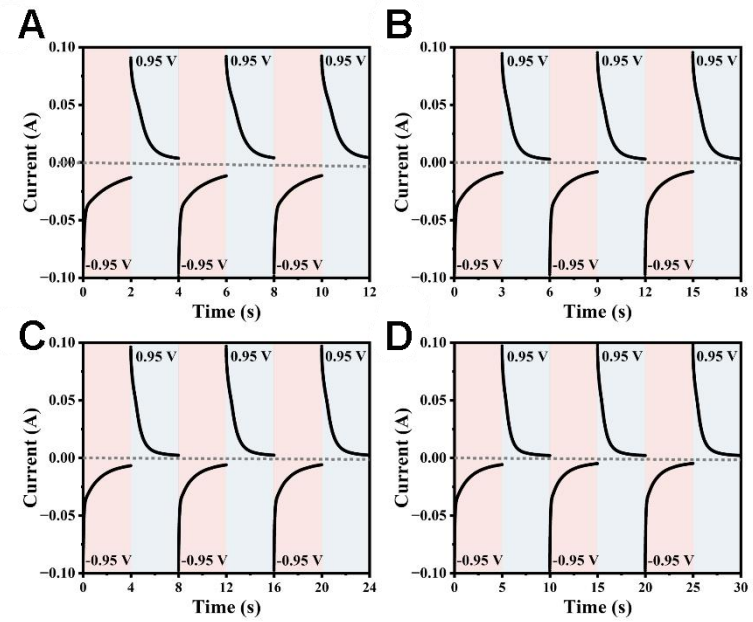

Supplementary Figure 16. Chronoamperometry curves of CAPode under alternating voltages of ± 0.95 V at different times of 2 s (A), 3 s (B), 4 s (C), and 5 s (D).

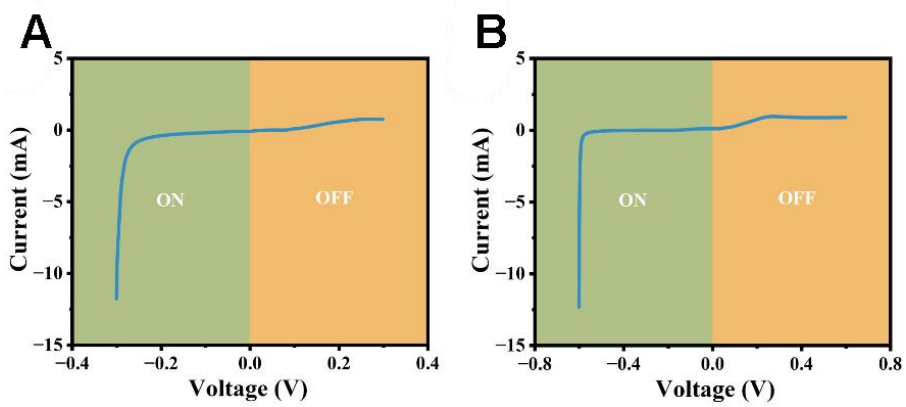

Supplementary Figure 17. I–V curves of CAPode under alternating external biases. (A) ± 0.3 V and (B) ± 0.6 V.

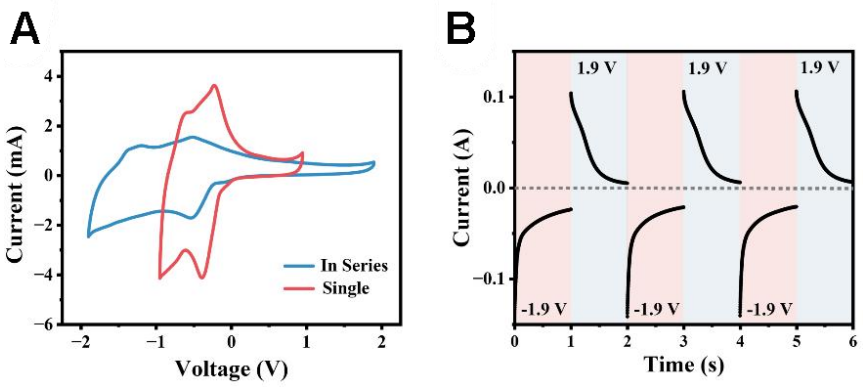

Supplementary Figure18. (A) CV curves and (B) chronoamperometry curves of two CAPodes connected in series under alternating voltages of ± 1.9 V, applied for 1 s.

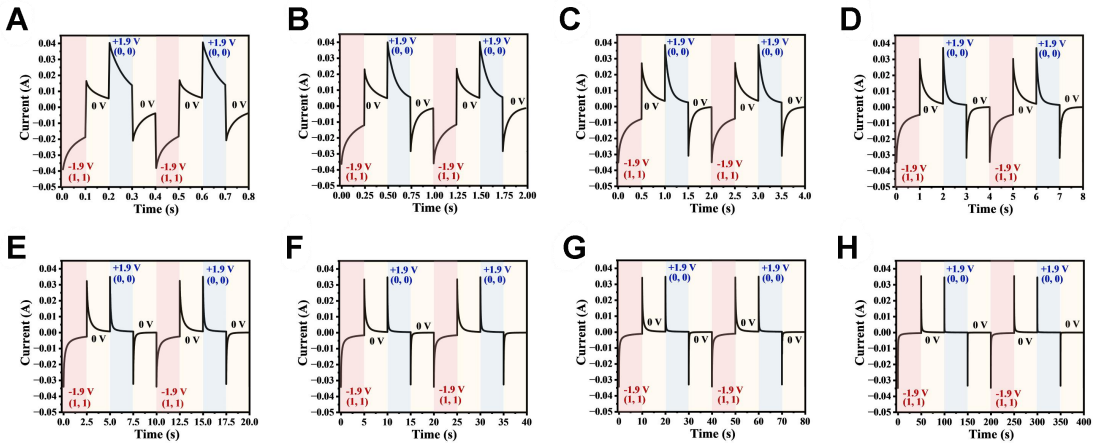

Supplementary Figure 19. Chronoamperometry curves of logic gate ("AND") under different inputs ((0,0) and (1,1) by alternating applied voltages of ±1.9 V for 0.1 s (A), 0.25 s (B), 0.5 s (C), 1 s (D), 2.5 s (E), 5 s (F), 10 s (G) and 50 s (H).

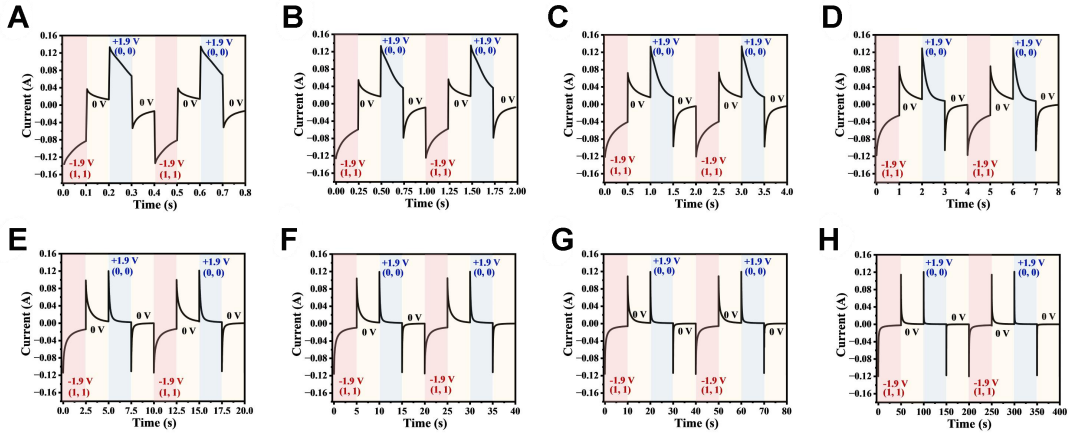

Supplementary Figure 20. Chronoamperometry curves of logic gate ("OR") under different inputs ((0,0) and (1,1) by alternating applied voltages of ±1.9 V for 0.1 s (A), 0.25 s (B), 0.5 s (C), 1 s (D), 2.5 s (E), 5 s (F), 10 s (G) and 50 s (H).

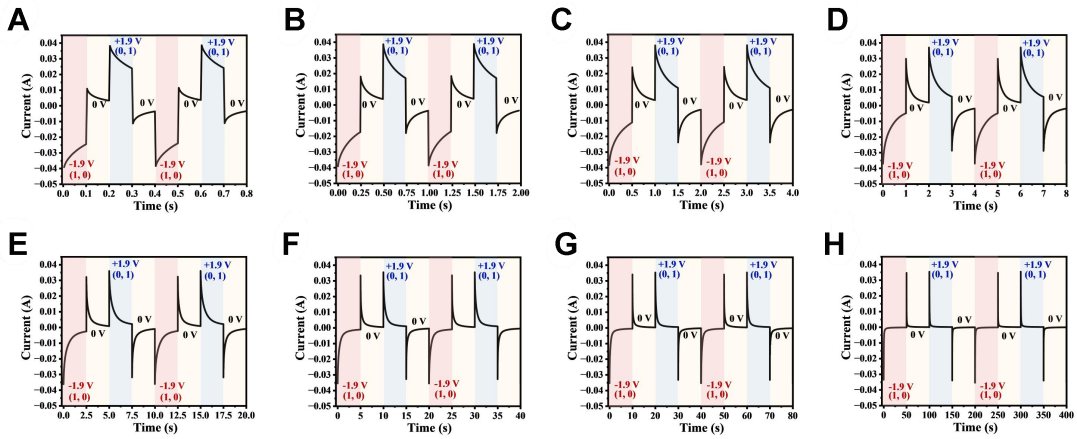

Supplementary Figure 21. Chronoamperometry curves of logic gate ("AND") under different inputs ((0,1) and (1,0) by alternating applied voltages of ±1.9 V for 0.1 s (A), 0.25 s (B), 0.5 s (C), 1 s (D), 2.5 s (E), 5 s (F), 10 s (G) and 50 s (H).

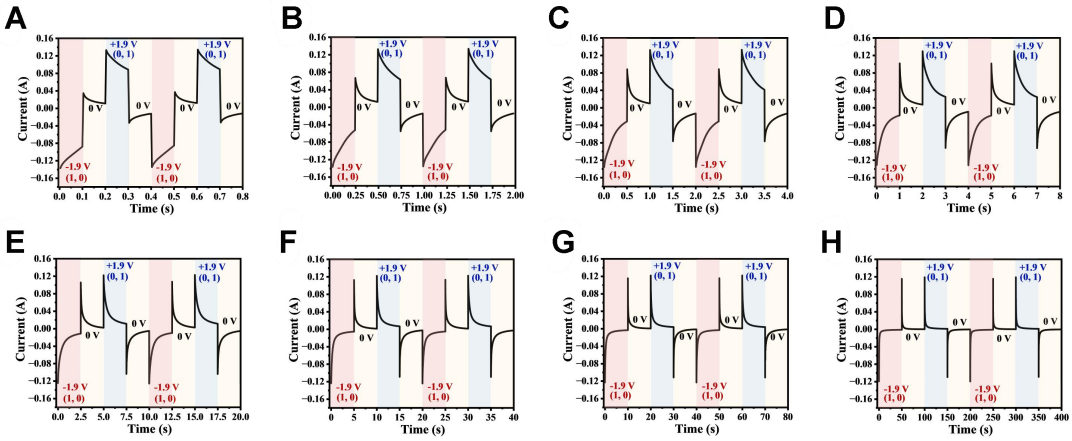

Supplementary Figure 22. Chronoamperometry curves of logic gate ("OR") under different inputs ((0,1) and (1,0) by alternating applied voltages of ±1.9 V for 0.1 s (A), 0.25 s (B), 0.5 s (C), 1 s (D), 2.5 s (E), 5 s (F), 10 s (G) and 50 s (H).

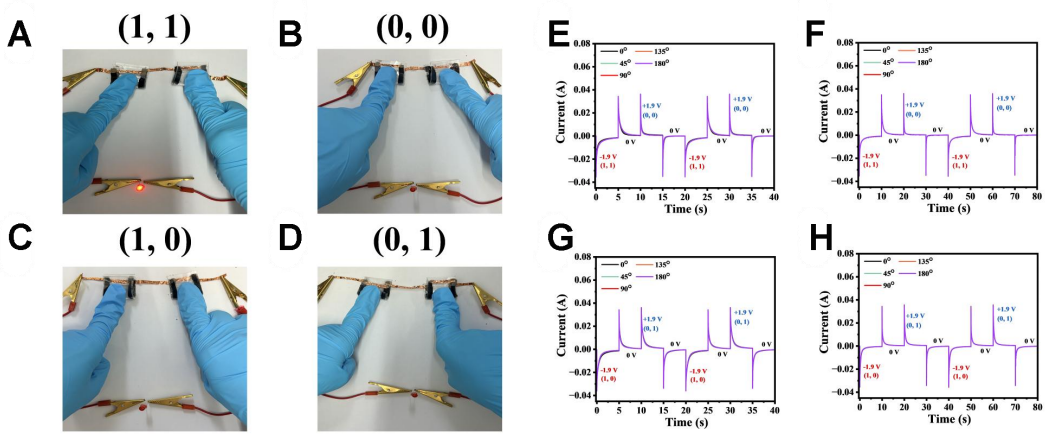

Supplementary Figure 23. The performance stability of logic gate "AND" under bending states. (A-D) Photographs by a digital camera of an "AND" gate with bending angle of 180° under (1, 1) (A), (0, 0) (B), (1, 0) (C) and (0, 1) (D) inputs, respectively. (E, F) Chronoamperometry curves of logic gate ("AND") under different inputs ((0,0) and (1,1)) by alternating voltages of ±1.9 V applied for 5 s (E) and 10 s (F) under different bending angles. (G, H) Chronoamperometry curves of logic gate ("AND") under different inputs ((0,1) and (1,0)) by alternating voltages of ±1.9 V applied for 5 s (G) and 10 s (H) after bending to different angles.

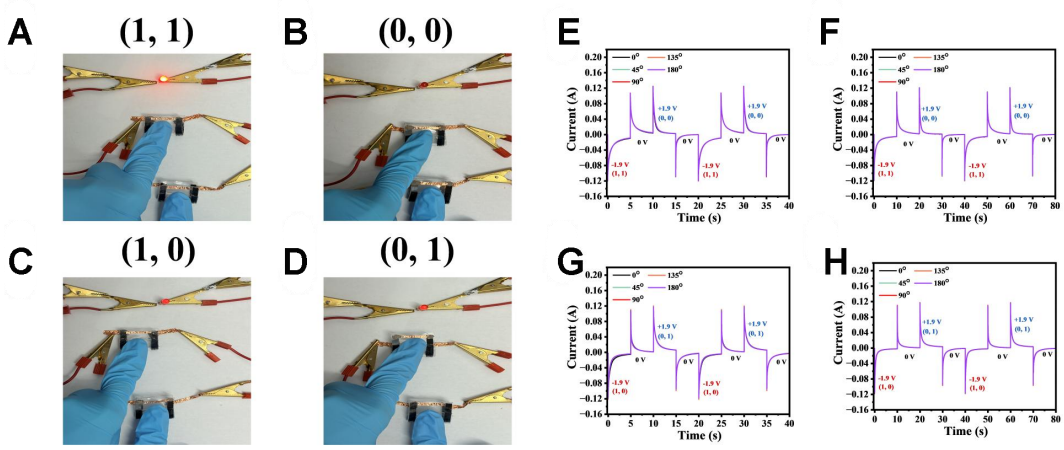

Supplementary Figure 24. The performance stability of logic gate "OR" under bending states. Photographs by a digital camera of an "OR" gate with bending angle of 180° under (1, 1) (A), (0, 0) (B), (1, 0) (C) and (0, 1) (D) inputs, respectively. (E, F) Chronoamperometry curves of logic gate ("OR") under different inputs ((0,0) and (1,1)) by alternating voltages of ±1.9 V, applied for 5 s (E) and 10 s (F) under different bending angles. (G, H) Chronoamperometry curves of logic gate ("OR") under different inputs ((0,1) and (1,0)) by alternating voltages of ±1.9 V, applied for 5 s (G) and 10 s (H) after bending to different angles.

References

[S1] Perdew, J. P. Burke, K. Ernzerhof,M. Generalized gradient approximation made simple. Phys Rev Lett, 1996, 77: 3865-3868.

[S2] Delley, B. An all-electron numerical method for solving the local density functional for polyatomic molecules. J Chem Phys, 1990, 92: 508-517.